Optical Operation by Chromophores Featuring 4,5-Dicyanoimidazole Embedded within Poly(methyl methacrylate) Matrices

ARTICLE *in* THE JOURNAL OF PHYSICAL CHEMISTRY A · SEPTEMBER 2010

Impact Factor: 2.69 · DOI: 10.1021/jp1047634 · Source: PubMed

Optical Operation by Chromophores Featuring 4,5-Dicyanoimidazole Embedded within Poly(methyl methacrylate) Matrices

J. Kulhánek,[†] F. Bureš,[†] A. Wojciechowski,[‡] M. Makowska-Janusik,[§] E. Gondek,[||] and I. V. Kityk*[,‡]

Institute of Organic Chemistry and Technology, Faculty of Chemical Technology, University of Pardubice, Studentská 573, Pardubice 53210, Czech Republic, Electrical Engineering Department, Czestochowa University of Technology, Armii Krajowej 17, Czestochowa, Poland, Institute of Physics, Jan Dlugosz University, Armii Krajowej 13/15, Czestochowa, Poland, and Institute of Physics, Cracow University of Technology, Podchorazych 1, Krakow, Poland

Received: May 25, 2010; Revised Manuscript Received: August 3, 2010

We have studied photoinduced absorption, birefringence, and optical second-harmonic generation in poly(methyl methacrylate) (PMMA) films doped by organic chromophores featuring 4,5-dicyanoimidazole in the weight content equal to 5%. The chromophores indicated as **IM1**−**IM6** were synthesized from 2-bromo-1-methylimidazole-4,5-dicarbonitrile by either nucleophilic substitution or Suzuki−Miyaura cross-coupling reaction. The samples were obtained as films of several micrometers thickness by the spin-coating method on a quartz substrate. Measurements of the optically induced birefringence were done by the Senarmont method at wavelength 1150 nm, and photoinduced absorption was studied in the spectral range 250−700 nm under optical treatment by 300 mW cw 532 nm laser. Photoinduced optical effects were studied by bicolor 1064 and 532 nm coherent laser pulses. The maximal changes were observed for the ratio between fundamental and writing beam intensities equal to about 7:1. To interpret the observed experimental measurements, theoretical simulations of photoinduced optical properties were performed by quantum chemical computational methods.

I. Introduction

A search for novel chromophores for optoelectronics and nonlinear optics (NLO) is one of the main goals of modern materials science and physics.[1−4] Their practical application requires not only the appropriate design but also the relevant macroscopic properties of newly established material. Therefore, the influence of different solvents on the NLO susceptibilities determining the efficiency of the laser transformation should be investigated. Due to this fact, the study of intermolecular interactions must be taken into consideration in host−guest materials. It is particularly important during the bicolor optical treatment,[5] where principal roles are played simultaneously by changes of absorption, refractive indices, and second- and third-order susceptibilities as well as the values of the dipole moments.

In this respect, organic dipolar π-conjugated molecules end-capped with donors and acceptors (D-π-A push−pull systems) featuring an intramolecular charge transfer were shown to be very efficient for NLO applications. Nonlinear optical properties of such organic chromophores can be easily tailored by variation of the appended donors and acceptors or by the elongation or shortening of the π-conjugated path.[6−8] Moreover, for successful fabrication of such compounds as NLO-active chromophores, high polarizability, good optical properties, solubility, and thermal stability are required. Hence, various heteroaromates were recently utilized as π-conjugated backbones. Among them, 4,5-dicyanoimidazole has been recognized as an easily accessible acceptor moiety and has found wide application in organic electronics[9] and composite materials possessing nonlinear optical properties.[10,11] In the present work the linear and nonlinear optical properties of 4,5-dicyanoimidazole derivatives are characterized. Generally we have focused on photoinduced changes of electronic molecular properties affected by the poly(methyl methacrylate) (PMMA) polymeric matrix. We try to explain the mechanism of photoinduced optical effects using experimental and quantum chemical simulation tools.

In section II, technology of chromophore synthesis and principal experimental details are presented. Section III describes principal details concerning quantum chemical methods implemented in performed calculations. The experimental and theoretical results with their comparison are described and summarized in section IV.

II. Chromophore Synthesis and Experimental Details

Recently, we have reported on the synthesis and properties of push−pull molecules based on 4,5-dicyanoimidazole derivatives, indicated as **IM1**−**IM6,** featuring a systematically extended π-conjugated system and a *N*,*N*-dimethylamino group as a strong donor.[12] The synthesis of the simplest imidazole, **IM1**, involves a bromine substitution in 2-bromo-1-methylimidazole-4,5-dicarbonitrile with dimethylamine in terms of nucleophilic aromatic substitution (S_NAr).[13] Moreover, the starting 2-bromo-1-methylimidazole-4,5-dicarbonitrile has further been utilized as a suitable electrophile in Suzuki−Miyaura cross-coupling. Such reaction with various *N*,*N*-dimethylamino-substituted π-linkers[14] provided directly the target compounds **IM2**−**IM6** with a systematically extended π-conjugated system. Thus, the *N*,*N*-dimethylamino donor was either connected directly to imidazole (**IM1**) or separated by 1,4-phenylene (**IM2**), (*E*)-phenylethynyl (**IM3**), biphenyl (**IM4**), (*E*)-phe-

* To whom correspondence should be addressed.
[†] University of Pardubice.
[‡] Czestochowa University of Technology.
[§] Jan Dlugosz University.
[||] Cracow University of Technology.

10.1021/jp1047634
Published on Web 08/17/2010

SCHEME 1: Synthesis and Molecular Structure of Chromophores IM1−IM6

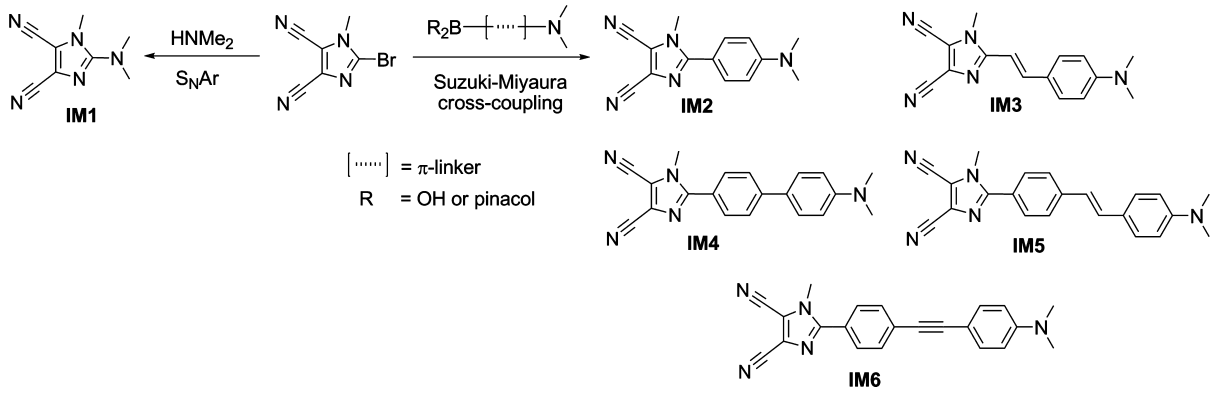

nylethenylphenyl (**IM5**), and phenylethynylphenyl (**IM6**) π-linkers, respectively. The reaction sequence and molecular structures of **IM1**−**IM6** chromophores are shown in Scheme 1.

Prepared chromophores were incorporated into the PMMA matrix by the spin-coating method on quartz substrates as described in ref 15. Their thickness was about 1 μm. The maximal content of chromophores in polymeric matrix was 4.9% (in weighting units). At the obtained level of doping, an aggregation of chromophores has been not yet observed. The homogeneity of their space distribution was controlled by spectrophotometer with spectral resolution about 1 nm within the 340−900 nm wavelengths. To study the second-order nonlinear optical effects, we have applied bicolor optical treatment at 1064 nm 10 ns laser wavelength with power density increasing steeply up to 300 MW/cm^2. Generally, the setup is similar to that described in ref 16.

III. Quantum Chemical Calculations

The electronic and optical properties of investigated molecules were calculated by applying ab initio and density functional theory (DFT) methods via GAMESS[17] and ADF[18] program packages, respectively. Before the exact quantum chemical calculation, the structural optimization of the considered molecule was performed. The total energy minimization was carried out by the ab initio method at restricted Hartree−Fock (RHF) level[19] with the standard 6-31G** basis set in C_1 symmetry. The gradient convergence tolerance was equal to 10^{-6} Hartree/Bohr by the quadratic approximation (QA)[20−22] method with the Hessian matrix updated during the optimization. The Hessian evaluation was performed to exclude the structures giving negative modes. The initial geometries of the **IM1**−**IM6** compounds have been also calculated at DFT implementation. The DFT calculations were performed with the standard triple-ζ basis sets extended by one polarized function (TZP), available in ADF package and described in the references cited there.[18] Core electrons of all atoms were kept frozen and any geometry restriction was not applied. The exchange−correlation (XC) energy in DFT model was calculated with the generalized gradient approximation (GGA). The Beck gradient correction of potential[23] was used to obtain the exchange part of the XC functional, and the Lee−Yang−Parr correction[24] was used to compute correlation part. The Hessian matrix was updated by the Broyden−Fletcher−Goldfarb−Shanno (BFGS)[25] method with the criterion for changes in the energy and gradient equal to 10^{-3} Hartrees and 10^{-2} Hartree/angstrom, respectively. It was found that the geometry of the **IM1**−**IM6** molecules calculated by DFT methods are consistent with those from the HF method. However, the bond lengths calculated by the HF method are little shorter than those obtained by DFT.

The electronic properties of isolated **IM1**−**IM6** molecules have been calculated at the self-consistent field restricted Hartree−Fock (SCF RHF) ab initio level by applying the standard 6-31++G** basis set as well as using the DFT method implemented in the ADF program and its ADF-RESPONSE module.[26] The excitation energies and hyperpolarizabilities calculated on the ab initio level were evaluated by configuration interaction single (CIS)[27,28] and time-dependent Hartree−Fock (TDHF)[29] methods. The SCF convergence criteria were chosen as relative density convergence equal to 10^{-12}, which corresponds to not more than 50 iterations. In both methods the Davidson algorithm was used for Hamiltonian diagonalization.[30−32] CIS and TDHF are the cheapest excited-state methods that include electron correlation via wave function methodology, but they are applicable to large molecules.

A conceptually different approach to include electron correlation is represented by the time-dependent density functional theory (TDDFT) method,[33] which is very modern and has become one of the most prominent methods for the calculation of excited states of medium-sized to large molecules. It is necessary to emphasize that TDDFT calculations reproduce well the experimental hyperpolarizability values for small molecules[34−37] but give unsatisfactory results for optical properties of long linear chains.[38] All parameters for the TDDFT calculations were applied as for geometry optimization have been chosen. The standard triple-ζ basis sets extended by two polarized functions (TZ2P) available in ADF were used with

TABLE 1: Electronic Parameters Obtained at ab initio and DFT Levels for Molecules IM1−IM6

	μ (D)		$\Delta E_{\mathrm{HOMO-LUMO}}$ (eV)		$\lambda_{\max}$ (nm)			
molecule	ab initio	DFT	ab initio	DFT	ab initio CIS	ab initio TDHF	DFT	$\lambda_{\exp}$ (nm)
IM1	9.12	9.20	11.11	3.18	212.9	226.3	344.8	293
IM2	11.77	12.53	9.87	2.56	230.3	242.3	455.9	316
IM3	12.67	13.94	9.07	2.24	271.5	285.6	477.5	381
IM4	12.18	13.20	9.26	2.09	242.2	254.0	577.3	346
IM5	12.84	14.54	8.68	1.96	276.0	290.1	597.4	380
IM6	12.78	14.45	8.82	2.02	266.6	280.8	582.8	364

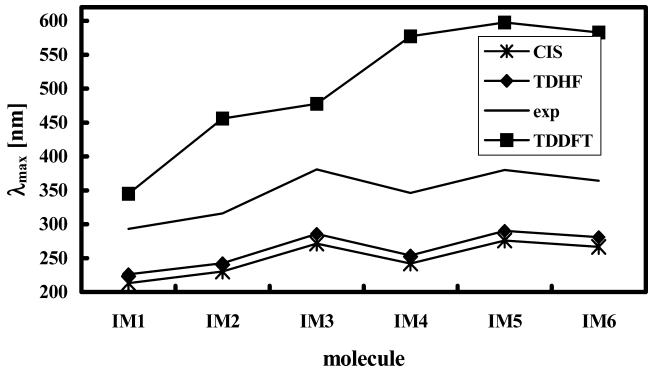

Figure 1. First UV−vis absorption peak λ_{max} position evaluation of **IM1**−**IM6** molecules (experimentally obtained and calculated by different methods).

core electrons frozen for all atoms. The SCF energy convergence criterion was chosen to be 10^{-12} Hartree. The excitation energies were calculated by the iterative Davidson method[39] with an accuracy of 10^{-12} Hartree. All the molecules were rotated to align maximal state ground dipole moment along the z-axis.

Moreover, by the ab initio CIS method, the photoinduced UV−vis absorption spectra were calculated for isolated **IM1**−**IM6** molecules. In order to obtain the intended purpose, the external field influence on the excited molecular electronic states were investigated. The strength of electric field used was equivalent to the 300 mW cw of 532 nm laser beam and was applied in *x*, *y*, and *z* directions of the molecular frame, successively. Then the UV−vis absorption changes obtained for different electric field directions were averaged. Subsequently, the nonilluminated and photoinduced UV−vis absorption spectra were compared and the oscillator strength's intensities of the corresponding wavelength were analyzed.

IV. Results and Discussion

All the investigated chromophores possess the *N*,*N*-dimethylamino donor group and 4,5-dicyanoimidazole acceptor groups joined by the π-conjugated phenyl-based systems. The spectral position of the charge transfer (CT) UV−vis absorption band depends on the length of the conjugated π-backbone. Electronic absorption spectra of investigated molecules **IM1**−**IM6** were obtained in CH_2Cl_2 solvent, and first UV−vis absorption peak positions are presented in Table 1. The λ_{max} value for all molecules appears between 293 and 381 nm.[12] It is far from the results obtained by computational simulations, performed at ab initio and DFT levels (see Table 1). The DFT calculations shift the absorption band to the red side, consequently with the extension of the π-conjugated system. However, the λ_{max} obtained by both ab initio methods used reflects a good tendency of the experimental absorption shift for particular molecules (Figure 1). One may see that the presence of π-conjugated bonds in investigated chromophores shifts the absorption band into the long-wave region and the CIS and TDHF methods reproduce this dependence very well compare to the TDDFT results. In general, excitation energies computed with ab initio method are usually overestimated and they are too large by about 0.5−2 eV compared with their experimental values;[40] however, the TDHF technique gives better values compared to the experimental ones than CIS. Concerning static dipole moment and highest occupied−lowest unoccupied molecular orbital (HOMO−LUMO) energy splitting values, both ab initio methods used give the same results (see Table 1). TDDFT yields substantial errors for CT excited states[41−43] where the excitation

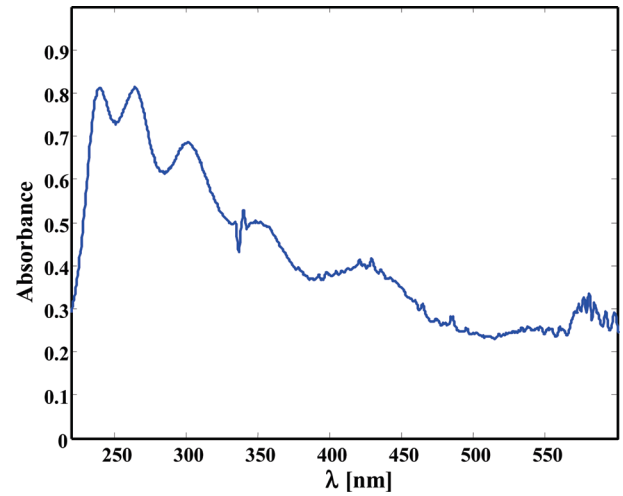

Figure 2. Typical absorption spectra of the composite films based on PMMA/IM(x) molecule.

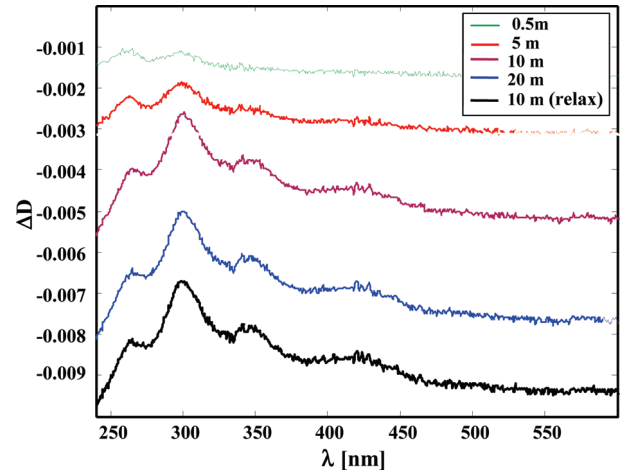

Figure 3. Photoinduced changes of absorption for **IM3** samples irradiated for different times by 300 mW cw laser beam with a relaxation process of 10 min (relax).

energies are usually drastically underestimated.[44] The potential energy curve does not exhibit the correct asymptote 1/*R*, where *R* corresponds to the distance between positive and negative charges of CT states. The wrong shape of the mentioned potential excludes the CT states from reliable calculations by the TDDFT method. In contrast to the TDDFT method, CIS and TDHF yield the correct 1/*R* behavior of the potential energy curve of CT states.

The obtained difference between calculated and experimentally obtained λ_{max} values may be a consequence of intermolecular interaction, which was here not taken into account and will be the subject matter of future work. The interaction between chromophores and solvent should give a red-side shift of absorption spectra, which is favorable for presented ab initio results. The UV−vis absorption spectrum obtained for one of the measured composites, based on investigated chromophores and PMMA polymeric matrix, is presented in Figure 2. One can see typical interference fringes superimposed on the absorption edge.

To explore the influence of laser irradiation on the spectral properties of chromophores, continuous-wave (cw) laser beam treatment studies on absorption UV−vis spectra were performed. Following Figure 3, one can clearly see an occurrence of at least three spectral maxima at 270, 305, and 360 nm possessing intensities that increase with the length of the sample's

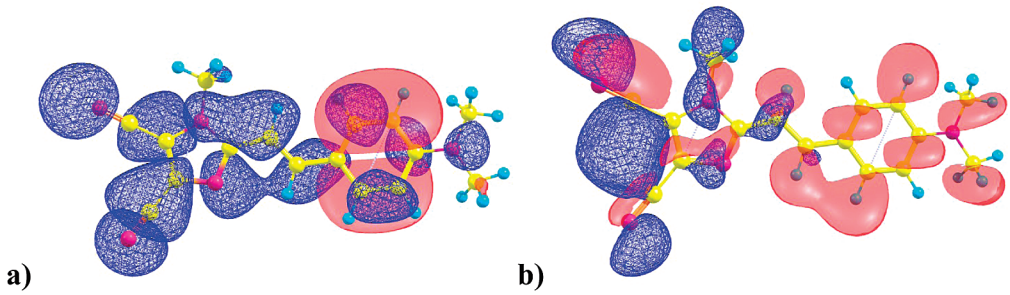

Figure 4. Molecular orbitals related to the absorption band creations of molecule **IM3** at (a) 219 nm and (b) 214 nm, calculated by the ab initio method. Blue shape indicates unoccupied molecular orbital; pink shape indicates occupied molecular orbital.

illumination. The more significant absorption enlargement was observed after the first 10 min of illumination. An additional larger spectral maximum occurs at 430 nm. This fact may indicate that the cw laser beam favors an occurrence of the photopolarized states, which substantially changes the occupation near the gap trapping levels. This relaxation does not show a quick photoinduced band decrease after 10 min. Such slow relaxation may indicate the substantial role of the long-lived metastable trapping levels in the processes observed here. At the same time, spectral peaks appearing at 270, 305, and 360 nm are probably connected to the increasing charge transfer mechanism contribution.

By comparison of Figures 2 and 3, the spectral peak located at 360 nm is the second electron excitation. It may be compared to the second absorption peak obtained theoretically at the ab initio level. Upon comparisin of the computational results obtained for irradiated and nonirradiated molecule **IM3**, the intensity of the second absorption peak is substantially changed. This peak is split into two peaks at 214 and 219 nm. The molecular orbitals, calculated by ab initio CIS method, involved in the mentioned electronic transition are presented in Figure 4. There are visualized molecular orbitals of the molecule **IM3** participating in electronic excitation responsible for the transition at 219 nm (Figure 4a) and 214 nm (Figure 4b). In pink are marked the occupied molecular orbitals, and in blue are marked the unoccupied ones corresponding to the mentioned transitions. One can clearly see that these two excitations are caused by charge transfer mechanism presence that is represented by the separation of the occupied and unoccupied molecular orbitals.

Laser beam irradiation has a completely different influence on samples **IM4** than molecule **IM3** (Figure 5). For **IM4**, the intensity of photoinduced absorption decreases. This is in principal agreement with Figure 6, where the theoretically obtained photoinduced absorption changes versus the first 10 excited states are presented. The drawing exhibits the changes calculated at ab initio CIS level for **IM4** and **IM5** molecules. One can see that for both molecules the intensity of photoinduced absorption decreases but the observed changes are not of the same magnitude. For **IM5** the changes are more pronounced than for **IM4**. For **IM4** one may observe a saturation of the photoinduced processes after 5 min of irradiation. The spectral positions noticed for molecule **IM4** are shifted up to 10 nm and the relaxation seems to be a bit quicker. It is crucial that for the **IM5** samples the illumination by laser beam creates some resonance at 270 nm (Figure 7). The photoinduced changes obtained for **IM4** are relatively low with respect to the **IM5** or **IM6** samples, which is in agreement with quantum chemical simulations (Figure 6). The relaxation for molecule **IM5** is also not too strong (Figure 7).

More pronounced changes in the absorption are observed for the samples **IM6** (see Figure 8). They have similar nature and

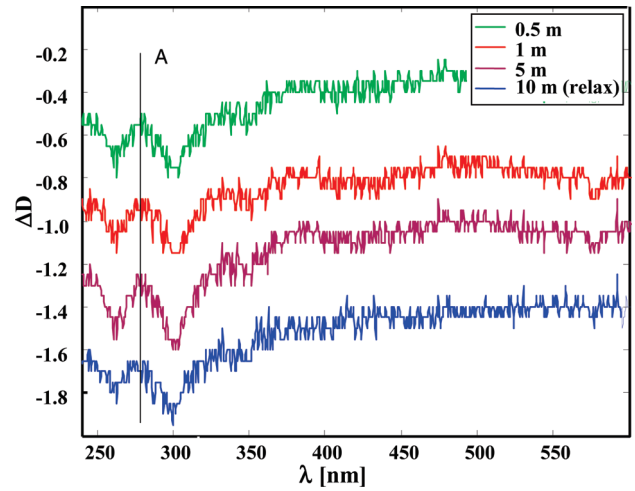

Figure 5. Photoinduced changes of absorption for **IM4** samples irradiated for different times by 300 mW cw laser treatment and relaxation.

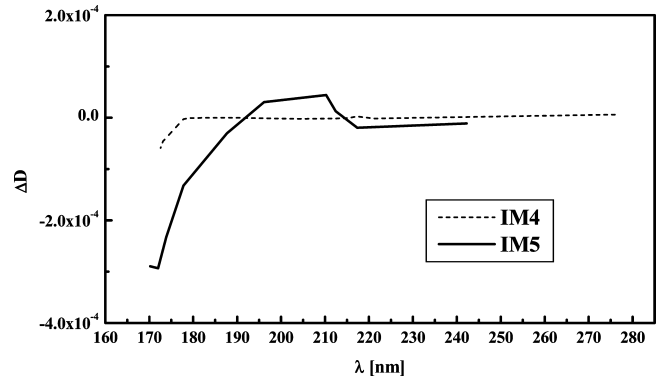

Figure 6. Photoinduced absorption changes obtained via CIS calculations for molecules **IM4** and **IM5**.

character to the data obtained for molecule **IM3** (Figure 3). One may clearly see an occurrence of at least four spectral maxima situated at 260, 301, 355, and 425 nm (Figure 8). Moreover, after 15 min following interruption of laser illumination, the observed maxima almost disappear. It confirms a possible influence of local thermoheating processes, which are superimposed on the photoinduced process. In this case the relaxation seems to be faster, because the maximum at 301 nm completely disappears. Calculated photoinduced changes of absorption spectra versus 10 excited states obtained for molecule **IM6** by the ab initio CIS method have similar behavior to those obtained for molecule **IM3** (Figure 9). The irregular changes are noticed for the entire spectral range. It is in contradiction to changes observed for molecules **IM4** and **IM5** (Figure 6). For these molecules the photoinduced changes are clearly observed for

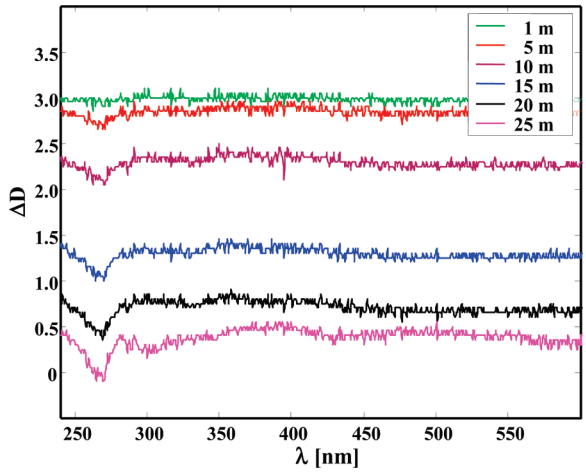

Figure 7. Photoinduced changes of absorption for **IM5** molecules irradiated for different times by 300 mW cw laser treatment.

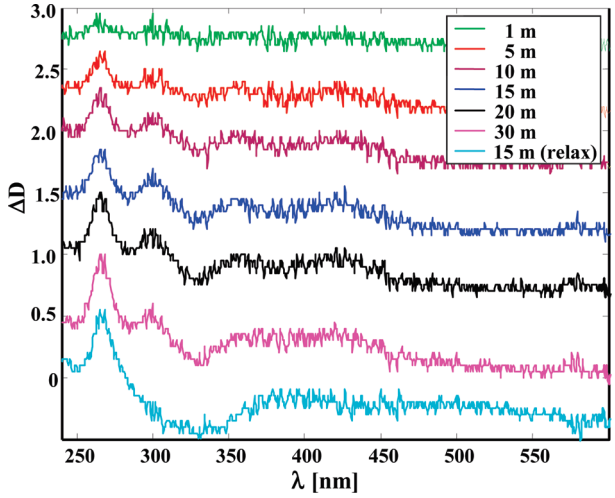

Figure 8. Photoinduced changes of absorption for **IM6** samples irradiated for different times by 300 mW cw laser treatment and relaxation.

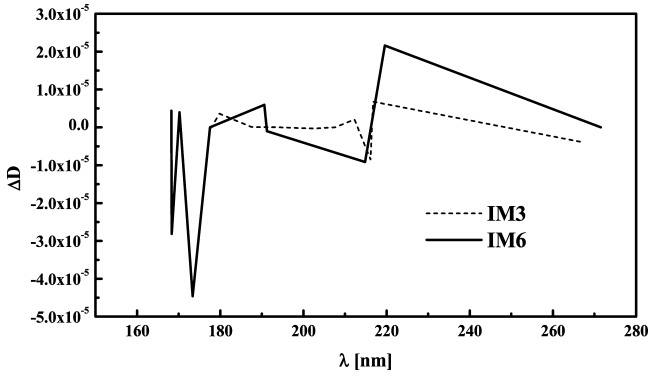

Figure 9. Photoinduced absorption changes (obtained at ab initio CIS level) for molecules **IM3** and **IM6**.

the low-wavelength spectra. However, the intensity of presented photoinduced absorption changes is more pronounced for molecules **IM4** and **IM5** than for **IM3** and **IM6**.

In Figure 10 are presented the dependences of the birefringence green cw laser treatment. One can see that the maximal magnitudes of the photoinduced birefringence for the probing wavelength 1150 nm were observed for the samples possessing the **IM6** chromophore and the results correlate well with the cw laser treatment. Moreover, a saturation of the birefringence

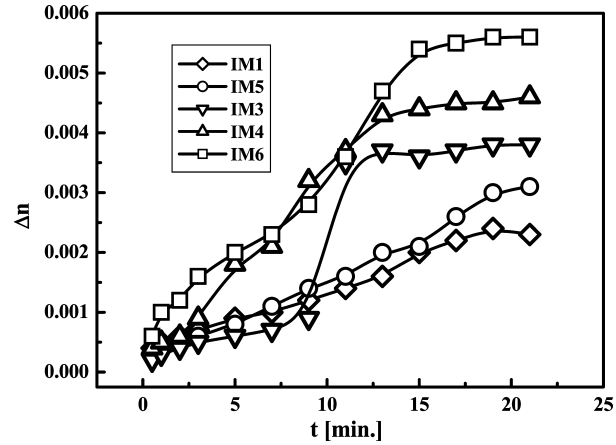

Figure 10. Dependence of photoinduced birefringence during the bicolor 1064 and 532 nm laser treatments vs duration of the cw optical treatment.

after 15 min of laser treatment is observed. The **IM4** samples during the first 10 min of the cw laser treatment show similar features and only with the longer times do they exhibit a saturation with the birefringence levels less than those of **IM6**. A similar tendency is shown by sample **IM3** and generally one can say that the behavior of these changes correlates well with the number of photoinduced resonances, which was shown also theoretically (Table 2). **IM1** and **IM5** show less changes of the birefringence and this also correlates with the lower values of the photoinduced optical oscillators for these composites. Mentioned processes show low relaxation. After 24 h the degree for birefringence decreases not more than 35%. The effect may be caused by occurrence of the photoinduced gratings due to occurrence of the noncentrosymmetry caused by simultaneous treatment with the two coherent laser beams. For this reason we have performed some calculations of the hyperpolarizablities applying the ab initio TDHF and TDDFT method (see Table 2). The DFT data are presented only for **IM1**−**IM3** molecules, because underestimation of the HOMO−LUMO energy splitting makes second-harmonic generation (SHG) calculations at λ = 1064 nm impossible for molecules **IM4**−**IM6**. For the molecules **IM4**−**IM6**, duplication of λ = 1064 nm is in the absorption range.

Following Table 2, one can see that the TDDFT method gives a smaller β_{av} value for **IM1** molecule compared to the data obtained by ab initio calculations. The results obtained for molecules **IM2** and **IM3** are reversed. It seems to be a consequence of the TDDFT method, which overestimates hyperpolarizability values for the rodlike molecules possessing π-conjugated bonds. For the molecule **IM1** the environmental influenced simulations were performed by taking into account the PMMA effect on the electronic properties of the chromophores. The calculations were carried out at the TDDFT level implementing the COSMO model.[45−47] The applied polymer−chromophore interaction increases the hyperpolarizability value up to β_{av} = 637 au. It is a double increase of the average SHG coefficient compared to the isolated molecules. It proves that the environmental effect is important in heterogeneous composite materials investigations as it was seen for the UV−vis absorption simulations.

By comparison of Figures 10 and 11, it is clearly seen that the optically induced birefringence and SHG achieve saturation at different durations of optical treatment. Both the birefringence and the SHG signal obtained for **IM6**-based composite reach the maximal values, which is in agreement with the theoretically calculated data (see Table 2). The different time indicates a

TABLE 2: First-Order Hyperpolarizability for Investigated IM1−IM6 Molecules at ab Initio and DFT Levels

$\beta(-2\omega;\omega,\omega)$ for $\lambda = 1064$ nm (atomic units)					
IM1	**IM2**	**IM3**	**IM4**	**IM5**	**IM6**
Ab Initio					
$\beta_x = 683$	$\beta_x = 2960$	$\beta_x = -550$	$\beta_x = -411$	$\beta_x = 3336$	$\beta_x = -2685$
$\beta_y = -118$	$\beta_y = 116$	$\beta_y = 7790$	$\beta_y = 4725$	$\beta_y = 10\,130$	$\beta_y = -8739$
$\beta_z = 572$	$\beta_z = 4820$	$\beta_z = 14\,818$	$\beta_z = 9652$	$\beta_z = 23\,688$	$\beta_z = 21\,542$
$\boldsymbol{\beta_{av} = 899}$	$\boldsymbol{\beta_{av} = 5657}$	$\boldsymbol{\beta_{av} = 16\,750}$	$\boldsymbol{\beta_{av} = 10\,754}$	$\boldsymbol{\beta_{av} = 25\,978}$	$\boldsymbol{\beta_{av} = 23\,401}$
DFT					
$\beta_x = 362$	$\beta_x = 5331$	$\beta_x = -1409$			
$\beta_y = -4$	$\beta_y = 320$	$\beta_y = 19\,233$			
$\beta_z = 342$	$\beta_z = 9452$	$\beta_z = 37\ 573$			
$\boldsymbol{\beta_{av} = 342}$	$\boldsymbol{\beta_{av} = 9452}$	$\boldsymbol{\beta_{av} = 37\,570}$			

different role for the photothermal effects which, following our estimation, give resulting heating not exceeding 5.6 K. For the other samples the tendency is a bit similar; however, the relative changes do not show exact proportionality to the ones obtained from calculations. This may indicate the contribution of higher-order multipole interactions to the effects as well as-contribution of the higher-order nonlinear optical effects.

V. Conclusions

During complex studies of photoinduced absorption, birefringence and photoinduced optical second-harmonic generation in the 4,5-dicyanoimidazole chromophores incorporated into the PMMA matrix, we have established that the behavior of these changes correlates well with the number of photoinduced absorption resonances, which also is confirmed theoretically. The magnitudes of the photoinduced absorption correlate well with the values of the photoinduced birefringence and SHG; however, sometimes there are some differences in their time-dependent behaviors.

The maximal photoinduced birefringence is observed for the **IM6** samples, which is in agreement with the theoretical calculations performed by TDDFT and ab initio TDHF method. The TDDFT method gives a smaller β_{av} value for **IM1** compared to the data obtained by ab initio calculations. The results obtained for molecules **IM2** and **IM3** are reversed. It seems to be a consequence of the TDDFT method, which overestimates hyperpolarizability values for the rodlike molecules possessing π-conjugated bonds. The performed complex studies show that the cw laser beam favors an occurrence of the photopolarized states that substantially changes the occupation near the gap trapping levels. This relaxation does not show a quick photo-induced band's decrease after 10 min. At the same time, spectral peaks appearing at 270, 305, and 360 nm are probably connected to the increasing charge transfer mechanism contribution. For the molecules **IM1**, the COSMO calculations were performed taking into account the environmental PMMA effect on the electronic properties of the chromophores. The polymer−chromophore interaction enhances the hyperpolarizability value up to $\beta_{av} = 637$ au. It is a double increase of the average SHG coefficient compared to the isolated molecules. This open a promising opportunity for the enhancement of the particular nonlinear optical susceptibilities.

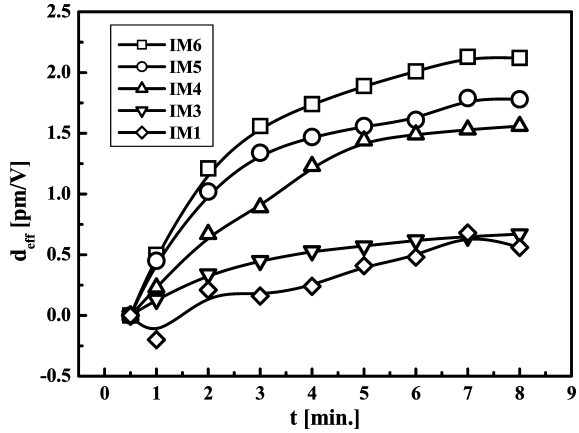

Figure 11. Dependence of the photoinduced SHG effect noticed at $\lambda = 1064$ nm obtained for investigated molecules.

Acknowledgment. J.K. and F.B. thank the Czech Science Foundation (203/08/0076) for financial support.

References and Notes

(1) Balakina, M. Y. *ChemPhysChem* **2006**, *7*, 2115.
(2) Hu, X.; Jiang, P.; Ding, C.; Yang, H.; Gong, Q. *Nat. Photonics* **2008**, *2*, 185.
(3) Kolev, T.; Koleva, B.; Kasperczyk, J.; Kityk, I. V.; Tkaczyk, S.; Spiteler, M.; Reshak, A. H.; Kuznik, W. *J. Mater. Science: Mater. Electron.* **2009**, *20*, 1073.
(4) Abbotto, A.; Beverina, L.; Manfredi, N.; Pagani, G. A.; Archetti, G.; Kuball, H.-G.; Wittenburg, C.; Heck, J.; Holtmann, J. *Chem.—Eur. J.* **2009**, *15*, 6175.
(5) Koścień, E.; Sanetra, J.; Gondek, E.; Jarosz, B.; Kityk, I. V.; Ebothe, J.; Kityk, A. V. *Opt. Commun.* **2004**, *242*, 401.
(6) Kuzyk, M. G. *J. Mater. Chem.* **2009**, *19*, 7444.
(7) May, J. C.; Biaggio, I.; Bureš, F.; Diederich, F. *Appl. Phys. Lett.* **2007**, *90*, 251106.
(8) Bureš, F.; Schweizer, W. B.; May, J. C.; Boudon, C.; Gisselbrecht, J.-P.; Gross, M.; Biaggio, I.; Diederich, F. *Chem.—Eur. J.* **2007**, *13*, 5378.
(9) Shin, R. Y. C.; Sonar, P.; Siew, P. S.; Chen, Z.-K.; Sellinger, A. *J. Org. Chem.* **2009**, *74*, 3293.
(10) Carella, A.; Centore, R.; Sirigu, A.; Tuzi, A.; Quatela, A.; Schutzmann, S.; Casalboni, M. *Macromol. Chem. Phys.* **2004**, *205*, 1948.
(11) Carella, A.; Centore, R.; Riccio, P.; Sirigu, A.; Quatela, A.; Palazzesi, C.; Casalboni, M. *Macromol. Chem. Phys.* **2005**, *206*, 1399.
(12) Kulhánek, J.; Bureš, F.; Pytela, O.; Mikysek, T.; Ludvík, J.; Rùžička, A. *Dyes Pigm.* **2010**, *85*, 57.
(13) O'Connell, J. F.; Parquette, J.; Yelle, W. E.; Wang, W.; Rapoport, H. *Synthesis* **1988**, *10*, 767.
(14) Kulhánek, J.; Bureš, F.; Ludwig, M. *Beilstein J. Org. Chem.* **2009**, *5*, 11.
(15) Migalska-Zalas, A.; Sofiani, Z.; Sahraoui, B.; Kityk, I. V.; Yuvshenko, V.; Fillaut, J.-L.; Perruchon, J.; Muller, T. J. J. *J. Phys. Chem. B* **2004**, *108*, 14942.
(16) Makowska-Janusik, M.; Gondek, E.; Kityk, I. V.; Wisla, J.; Sanetra, J.; Danel, A. *Chem. Phys.* **2004**, *306*, 265.
(17) Schmidt, M. W.; Baldridge, K. K.; Boatz, J. A.; Elbert, S. T.; Gordon, M. S.; Jensen, J. H.; Koseki, S.; Matsunaga, N.; Nguyen, K. A.; Su, S. J.; Windus, T. L.; Dupuis, M.; Montgomery, J. A. *J. Comput. Chem.* **1993**, *14*, 1347–1363.
(18) (a) te Velde, G.; Baerends, E. J.; *J. Comput. Phys.* **1992**, *99*, 84. (b) Baerends, E. J.; Berces, A.; Bo, C.; Boerribter, P. M.; Cavallo, L.; Deng, L.; Dickson, R. M.; Ellis, D. E.; Fan, L.; Fisher, T. H.; Fonseca Guerra, C.; van Gisbergen, S. J. A.; Groeneveld, J. A.; Gritsenko, O. V.; Harris, F. E.; van den Hoek, P.; Jacobsen, H.; van Kessel, G.; Kootstra, F.; van Lenthe, E.; Om, V. P.; Relasesinga, Philipsen, R. T. H.; Post, D.; Pye, C. C.;

Ravenek, W.; Ros, P.; Schipper, P. R. T.; Schreckenbach, G.; Snijders, J. G.; Sola, M.; Swerhone, D.; te Velde, G.; Vernooijs, P.; Versluis, L.; Visser, O.; van Wezenbeek, E.; Wiesenekker, G.; Wolff, S. K.; Woo, T. K.; Ziegler, T. ADF Program System, release 2004.01.

(19) Almlof, J.; Faegri, K., Jr.; Korsell, K. K. *J. Comput. Chem.* **1982**, *3*, 385.

(20) Baker, J. *J. Comput. Chem.* **1986**, *7*, 385.

(21) Helgaker, T. *Chem. Phys. Lett.* **1991**, *182*, 305.

(22) Culot, P.; Dive, G.; Nguyen, V. H.; Ghuysen, M. J. *Theor. Chim. Acta* **1992**, *82*, 189.

(23) Becke, A. D. *Phys. Rev. A* **1988**, *38*, 3098.

(24) Lee, C.; Yang, W.; Parr, R. G. *Phys. Rev. B* **1988**, *37*, 785.

(25) Head, J. D.; Zerner, M. C. *Chem. Phys. Lett.* **1995**, *122*, 264.

(26) van Gisbergen, S. J. A.; Snijders, J. G.; Berends, E. J. *Comput. Phys.* **1999**, *118*, 119.

(27) Kutzelnigg, W. *J. Mol. Struct. (THEOCHEM)* **1988**, *181*, 33.

(28) Head-Gordon, M.; Rico, R. J.; Oumi, M.; Lee, T. J. *Chem. Phys. Lett.* **1994**, *219*, 21.

(29) Sekino, H.; Bartlett, R. J. *J. Chem. Phys.* **1986**, *85*, 976.

(30) Foresman, J. B.; Head-Gordon, M.; Pople, J. A.; Frisch, M. J. *J. Phys. Chem.* **1992**, *96*, 135.

(31) Shroll, R. M.; Edwards, W. D. *Int. J. Quantum Chem.* **1997**, *63*, 1037.

(32) Webb, S. P. *Theor. Chem. Acc.* **2006**, *116*, 355.

(33) Gross, E. K. U.; Kohn, W. *Adv. Quantum Chem.* **1990**, *21*, 255.

(34) van Gisbergen, S. J. A.; Snijders, J. G.; Boerends, E. J. *J. Chem. Phys.* **1998**, *109*, 10644.

(35) Cohen, J. A.; Handy, N. C.; Tozen, D. J. *J. Chem. Phys. Lett.* **1999**, *303*, 391.

(36) Riccardi, G.; Rosa, A.; van Gisbergen, S. J. A.; Baerends, E. J. *J. Phys. Chem. A* **2000**, *104*, 635.

(37) te Velde, G.; Bickelhaupt, F. M.; Baerends, E. J.; Fonseca Guerra, C.; van Gisbergen, S. J. A.; Snijders, J. G.; Ziegler, T. *J. Comput. Chem.* **2001**, *22*, 931.

(38) van Faassen, Boeij, P. L.; van Leeuwen, R.; Berger, J. A.; Snijders, J. G. *Phys. Rev. Lett.* **2002**, *88*, 186401.

(39) Davidson, E. R. *J. Comput. Phys.* **1975**, *17*, 87.

(40) Hirata, S.; Head-Gordon, M.; Bartlett, R. J. *J. Chem. Phys.* **1999**, *111*, 10774.

(41) Dreuw, A.; Weisman, J. L.; Head-Gordon, M. *J. Chem. Phys.* **2003**, *119*, 2943.

(42) Dreuw, A.; Fleming, G. R.; Head-Gordon, M. *J. Chem. Phys. B* **2003**, *107*, 6500.

(43) Sobolewski, A. L.; Domcke, W. *Chem. Phys.* **2003**, *294*, 73.

(44) Dreuw, A.; Head-Gordon, M. *Chem. Rev.* **2005**, *105*, 4009.

(45) Klamt, A.; Schüürmann, G. *J. Chem. Soc., Perkin Trans.* **1993**, *2*, 799.

(46) Klamt, A. *J. Phys. Chem.* **1995**, *99*, 2224.

(47) Klamt, A.; Jones, V. *J. Chem. Phys.* **1996**, *105*, 9972.

JP1047634